One-loop electroweak radiative corrections to polarized $e^+e^- \to ZZ$ process

S. Bondarenko[*]
Bogoliubov Laboratory of Theoretical Physics, Joint Institute for Nuclear Research, Dubna, 141980 Russia

Ya. Dydyshka[†], L. Kalinovskaya, R. Sadykov, and V. Yermolchyk[†]
Dzhelepov Laboratory of Nuclear Problems, Joint Institute for Nuclear Research, Dubna, 141980 Russia

(Received 29 September 2023; accepted 25 December 2023; published 29 February 2024)

In the paper we recalculate and discuss high-precision theoretical predictions for cross sections of the process $e^+e^- \to ZZ$. We assume a complete one-loop implementation and a possibility of estimating the initial state polarizations, as well as the full-phase calculation. Numerical results are provided by our Monte Carlo tools `MCSANC` integrator and `ReneSANCe` generator for typical energies and degrees of polarization of ILC and CLIC projects in two $\alpha(0)$ and G_μ electroweak schemes.

DOI: 10.1103/PhysRevD.109.033012

I. INTRODUCTION

The process of Z pair production together with the process $e^+e^- \to \gamma Z$ is the main background for the reaction $e^+e^- \to ZH$ at the center-of-mass system (c.m.) energy of 250 GeV in the Higgs boson measurement method. This method should identify Higgs boson events independent of the decay mode allowing the measurement of the total cross section for Higgs production. Recently, we have estimated theoretical uncertainties for the polarized annihilation $e^+e^- \to ZH$ [1,2] and $e^+e^- \to \gamma Z$ [3] in the same way, i.e., by describing the one-loop level using the massive helicity approach in the full phase space.

To our knowledge, the QED and electroweak (EW) corrections to the unpolarized Z boson pair production have previously been calculated only in [4–6].

In this article we revise the uncertainties in the theoretical interpretation of the process

$$e^+(p_1,\chi_1) + e^-(p_2,\chi_2) \to Z(p_3,\chi_3) + Z(p_4,\chi_4)(+\gamma(p_5,\chi_5)). \quad (1)$$

For the virtual part, we discussed analytic expressions for the covariant amplitude, tensor structures, and helicity amplitudes and presented them in a compact form in [7]. The contribution of the hard real photon emission is obtained by direct squaring of the matrix element.

In this paper we extend the research and evaluate the complete one-loop corrections supplemented by higher-order QED contributions in the leading logarithmic approximation (LLA) by the structure function approach [8]. The impact of the initial-state radiation (photons and pairs) is analyzed order by order. We used known expressions for contributions of the collinear electron structure function of the orders $\mathcal{O}(\alpha^n L^n)_{\gamma,\text{pairs}}$, $n = 2$–4 for photons and pairs [2]. Based on this background we analyze the size of the radiative corrections and different higher-order contributions. Presumably, to evaluate ISR QED corrections the exponentiated procedure is more suitable for Monte Carlo simulations, while the order-by-order one can be used for benchmarks and cross-checks. We intend to use a parton shower for QED based on quantum density matrix factorization that was proposed by Nagy-Soper [9,10]. This approach allows resummation of all collinear logarithms taking into account spin correlations and can be a valuable alternative for older YFS-based algorithms [11,12].

This work explores the influence of the initial beam polarization at the planned experiments on ILC, FCC, CEPC for the reaction $e^+e^- \to ZZ$ with both Z bosons on-mass shell. Since this issue has not been studied before, we decided to investigate it carefully and to publish the results missing in literature.

We consider a narrow-width cascade using Born and one-loop $e^+e^- \to ZZ$ and $Z \to \mu^+\mu^-$ results as a rough estimation of the partial $e^+e^- \to ZZ \overset{\text{n.w.}}{\to} 2\mu^+2\mu^-$ channel. The gauge-invariant analytical results of initial state QED corrections to off-shell vector boson pair production were given in [13,14]. The corrections in which the two

[*]bondarenko@jinr.ru
Also at Dubna State University, Dubna 141980, Russia.
[†]Also at Institute for Nuclear Problems, Belarusian State University, Minsk, 220006 Belarus.

W- or Z-boson resonances are not independent due to the exchange of soft photons between the different subprocesses (nonfactorizable corrections) are estimated in [15].

Whenever possible, we compare our results with those described in literature. Polarized tree-level cross sections (the Born and hard photon bremsstrahlung) are compared with the CalcHEP [16] and WHIZARD [17,18] results; the weak and QED parts, with [4]; the NLO level, with the results [6].

Numerical results are presented for the total and differential cross sections that are functions of the cosine of the scattering angle, and for the relative corrections in the $\alpha(0)$ and G_μ EW schemes with an estimation of the polarization effects of the initial states.

All calculations were carried out using the `MCSANC` integrator and the `ReneSANCe` generator [19] which allow to evaluate the arbitrary differential cross sections and separate particular contributions.

The article is organized as follows. Section II describes the stage of the calculation of the polarized cross sections at the complete one-loop EW level. We consistently set out the relevant components of the one-loop cross section within the helicity approach. In Sec. III, the tuned comparison with third-party codes is presented for tree and one-loop levels. The corresponding numerical results are given for the total, differential cross sections, relative corrections with an estimation of polarization effects, left-right asymmetry and narrow-width approximation for decay channel.

In Sec. IV the discussion and conclusions are given.

II. DIFFERENTIAL CROSS SECTION

The cross section of any reaction e^+e^- annihilation with longitudinal electron beam polarizations P_{e^-} and positron beam polarization P_{e^+} is computed from the four possible pure helicity cross sections. To study the case of the longitudinal polarization with degrees P_{e^+} and P_{e^-} we make a formal application of Eq. (1.15) from [20]

$$\sigma(P_{e^+},P_{e^-})=\frac{1}{4}\sum_{\chi_1\chi_2}(1+\chi_1P_{e^+})(1+\chi_2P_{e^-})\sigma_{\chi_1\chi_2}, \quad (2)$$

where $\chi_i=-1(+1)$ corresponds to the particle i with the left (right) helicity.

The cross section of the process at the one-loop level can be divided into four parts:

$$\sigma^{\text{one-loop}}_{\chi_1\chi_2}=\sigma^{\text{Born}}_{\chi_1\chi_2}+\sigma^{\text{virt}}_{\chi_1\chi_2}(\lambda)+\sigma^{\text{soft}}_{\chi_1\chi_2}(\lambda,\bar{\omega})+\sigma^{\text{hard}}_{\chi_1\chi_2}(\bar{\omega}). \quad (3)$$

Here σ^{Born} is the Born cross section, $\sigma^{\text{virt}}=\sigma^{\text{QED}}+\sigma^{\text{weak}}$ is the contribution of virtual (loop) corrections, $\sigma^{\text{soft(hard)}}$ is the soft (hard) photon emission contribution (the hard photon energy $E_\gamma>\bar{\omega}=\omega\sqrt{s}/2$). We divide the virtual part into two gauge invariant subsets: σ^{QED} and σ^{weak}. To the QED contribution we refer all diagrams in which there is an exchange of at least one photon. The rest is the weak part. Auxiliary parameters λ ("photon mass") and $\bar{\omega}$ (soft-hard separator) are canceled after summation. The cancellation is controlled numerically by calculating the cross section at several values of the λ and $\bar{\omega}$ parameters. When calculating the emission of real photons we keep the electron masses to regularize the collinear divergences.

III. NUMERICAL RESULTS AND COMPARISONS

For numerical evaluations we used the following setup of input parameters:

$$\begin{aligned}
&\alpha^{-1}(0)=137.035999084,\\
&M_W=80.379\ \text{GeV}, \qquad M_Z=91.1876\ \text{GeV},\\
&M_H=125\ \text{GeV},\\
&\Gamma_Z=2.4952\ \text{GeV}, \qquad m_e=0.51099895\ \text{MeV},\\
&m_\mu=0.1056583745\ \text{GeV}, \qquad m_\tau=1.77686\ \text{GeV},\\
&m_d=0.083\ \text{GeV}, \qquad m_s=0.215\ \text{GeV},\\
&m_b=4.7\ \text{GeV}, \qquad m_u=0.062\ \text{GeV},\\
&m_c=1.5\ \text{GeV}, \qquad m_t=172.76\ \text{GeV}, \quad (4)
\end{aligned}$$

and set of c.m. energies

$$\sqrt{s}=250,500,\ \text{and}\ 1000\ \text{GeV}. \quad (5)$$

The following longitudinally polarized states are considered:

$$\begin{aligned}
(P_{e^+},P_{e^-})=&(0,0),\quad (-1,+1),\quad (+1,-1),\\
&(-0.3,+0.8),\quad (+0.3,-0.8),\\
&(0,+0.8),\quad (0,-0.8), \quad (6)
\end{aligned}$$

where (P_{e^+},P_{e^-}) are the positron and electron beam polarizations.

Original calculations were performed without angular cuts, while for comparison we used the cuts from considered papers.

A. Comparison with other codes

1. The tree level

The agreement in 5 digits was found for the results for the Born cross section with the codes CalcHEP and WHIZARD, so we omitted the corresponding table.

The results of the comparison for the hard photon bremsstrahlung with the only cut on the photon energy $E_\gamma>\bar{\omega}=10^{-4}\sqrt{s}/2$ within the $\alpha(0)$ EW scheme for unpolarized and fully polarized initial beams are given in Table I. The agreement within four digits is demonstrated.

TABLE I. The tuned triple comparison between the SANC (first line), CalcHEP (second line), and WHIZARD (third line) hard photon bremsstrahlung contributions σ^{hard} (fb) to polarized $e^+e^- \to ZZ(\gamma)$ scattering for various degrees of polarization and energies.

P_{e^+}, P_{e^-}	0,0	$-1,+1$	$+1,-1$
	$\sqrt{s} = 250$ GeV		
S	985.3(1)	1165.8(1)	2774.2(1)
C	985.2(1)	1165.7(1)	2774.1(1)
W	985.4(1)	1166.0(1)	2774.3(1)
	$\sqrt{s} = 500$ GeV		
S	433.1(1)	511.7(1)	1217.8(1)
C	433.1(1)	511.9(1)	1217.6(1)
W	433.2(1)	511.7(1)	1218.1(1)
	$\sqrt{s} = 1000$ GeV		
S	173.0(1)	204.2(1)	486.0(1)
C	173.0(1)	204.3(1)	486.1(1)
W	173.0(1)	204.2(1)	486.0(1)

2. The one-loop level

Comparison with [4]. We also made a separate comparison between SANC and [4] for the QED virtual part with the soft photon contribution $\delta^{\text{virt+soft}}$ and the virtual weak contribution to the NLO calculations δ^{weak}. In our previous paper [21] we found an excellent agreement with the virtual weak contribution numbers from the fourth column in Table I [4] with original setups and cuts. In this research we additionally compare the corresponding angular distributions of the QED virtual part with soft photon relative corrections $\delta^{\text{virt+soft}}$ (Fig. 1) and the virtual weak relative corrections δ^{weak} (Fig. 2). The calculated A_{LR} asymmetry of the QED and weak virtual parts with the soft photon contribution is presented in Fig. 3. The results show very good agreement with those given in Figs. 9, 11, and 12 of [4].

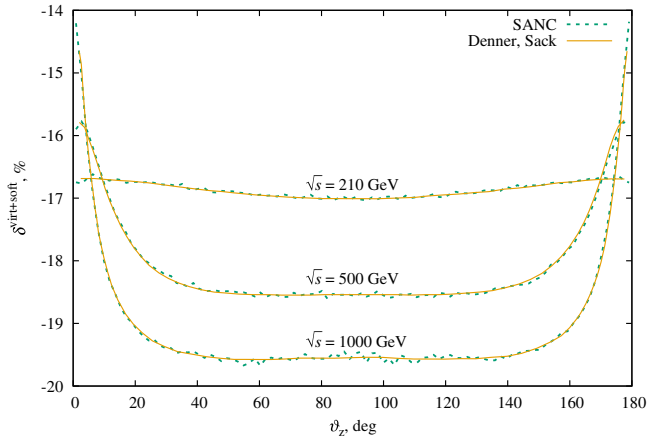

FIG. 1. Tuned comparison between the SANC and [4] results for the relative QED corrections $\delta^{\text{virt+soft}}(\omega = 0.1)$.

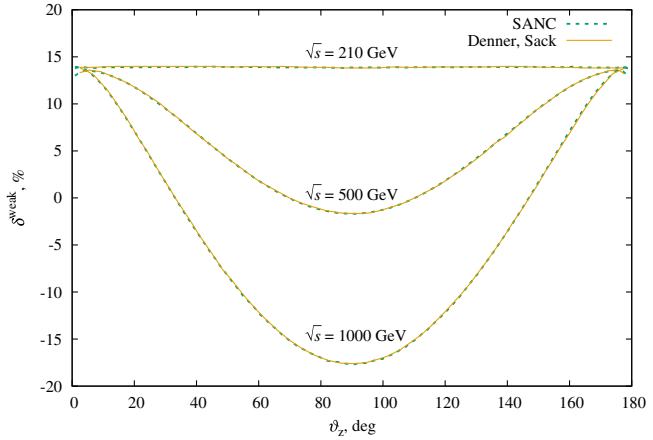

FIG. 2. Tuned comparison between the SANC and [4] results for the relative weak corrections δ^{weak}.

Comparison with [6]. In [6] the calculations of complete one-loop results of the process (1) are given with allowance for the longitudinal polarization of the initial beams. We compare our results with those obtained in [6] with the original cuts and input parameters for the unpolarized case.

At the tree level (Born and hard-photon bremsstrahlung cross sections) we agree with the results in Table I [6] within 4–5 digits.

For the NLO results, we found a difference in the total relative corrections at the c.m. energies (5), namely, $-1.20(1)\%$, $+6.77(1)\%$, $+6.54(1)\%$, respectively (should be compared with Table II of [6]).

Since the definitions of QED and weak subsets of the one-loop diagrams differ in the SANC system (see, for example, [22,23]) and those given in [6], it is impossible to compare the separate QED and weak contributions. We also see a difference in the angular distributions of the unpolarized cross sections.

It should also be noted that in [6] the inconsistent definition of the G_μ EW scheme is used. To avoid double counting in the G_μ scheme, the subtraction of the parameter

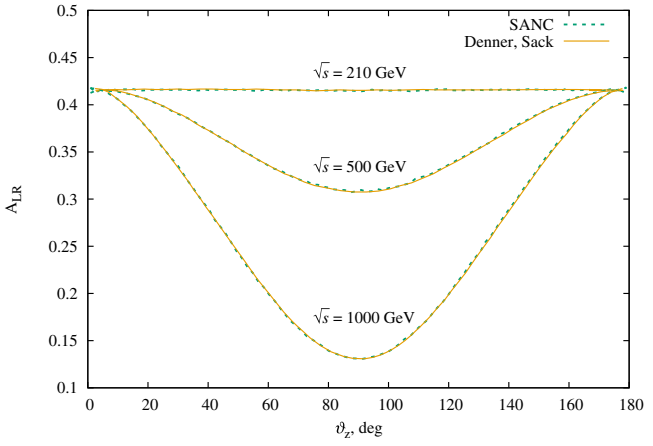

FIG. 3. Tuned comparison between the SANC and [4] results for A_{LR}.

TABLE II. Integrated Born and one-loop cross sections and relative corrections for unpolarized and polarized initial beams at the c.m. energies (5).

P_{e^+}, P_{e^-}	0, 0	−1, +1	+1, −1	+0.3, −0.8	−0.3, +0.8	0, −0.8	0, +0.8
			$\sqrt{s} = 250$ GeV				
$\sigma^{\rm Born}$, pb	1.0198(1)	1.2070(1)	2.8722(1)	1.7225(1)	0.80661(1)	1.3529(1)	0.68675(1)
$\sigma^{\rm NLO}$, pb	1.0087(1)	1.4717(1)	2.5625(1)	1.5508(1)	0.95079(3)	1.2270(1)	0.79067(3)
$\delta^{\rm NLO}$, %	−1.08(1)	21.93(1)	−10.78(2)	−9.97(1)	17.88(1)	−9.30(1)	15.14(1)
$\delta^{\rm QED}$, %	−1.36(1)	−1.39(1)	−1.39(1)	−1.38(1)	−1.37(1)	−1.37(1)	−1.34(1)
$\delta^{\rm weak}$, %	0.29(2)	23.32(1)	−9.39(1)	−8.59(1)	19.24(2)	−7.93(1)	16.48(2)
			$\sqrt{s} = 500$ GeV				
$\sigma^{\rm Born}$, pb	0.38530(1)	0.45604(1)	1.08518(2)	0.65079(1)	0.30476(1)	0.51115(1)	0.25947(1)
$\sigma^{\rm NLO}$, pb	0.41320(2)	0.69420(2)	1.04592(3)	0.63358(3)	0.39058(2)	0.50159(2)	0.32486(2)
$\delta^{\rm NLO}$, %	7.24(1)	32.49(1)	−3.62(1)	−2.65(1)	28.16(1)	−1.87(1)	25.20(1)
$\delta^{\rm QED}$, %	9.49(1)	9.32(1)	9.32(1)	9.40(1)	9.49(1)	9.46(1)	9.58(1)
$\delta^{\rm weak}$, %	−2.25(1)	23.17(1)	−12.94(1)	−12.05(1)	18.67(1)	−11.33(1)	15.62(1)
			$\sqrt{s} = 1000$ GeV				
$\sigma^{\rm Born}$, pb	0.14044(1)	0.16622(1)	0.39556(2)	0.23722(1)	0.11108(1)	0.18631(1)	0.94571(1)
$\sigma^{\rm NLO}$, pb	0.15614(2)	0.23058(1)	0.39217(2)	0.23784(2)	0.14896(1)	0.18846(2)	0.12382(1)
$\delta^{\rm NLO}$, %	11.17(1)	38.72(1)	−0.85(1)	0.27(1)	34.09(2)	1.16(1)	30.92(2)
$\delta^{\rm QED}$, %	15.90(1)	15.58(1)	15.59(1)	15.73(1)	15.89(1)	15.82(1)	16.06(1)
$\delta^{\rm weak}$, %	−4.72(1)	23.13(1)	−16.43(1)	−15.46(1)	18.21(2)	−14.67(1)	14.87(2)

Δr in a one-loop precision should be done along with changing the fine structure constant $\alpha(0) \to \alpha_{G_\mu}$ (see, for instance, [23,24]). This gives about $-(5-6)\%$ to the relative corrections of the virtual contribution in the G_μ EW scheme.

B. Total cross sections

Corresponding unpolarized/polarized results for the Born and complete one-loop EW cross sections (in picobarns), as well as for relative corrections, are presented in Table II. Relative corrections δ^i are computed as the ratios (in percent) of the corresponding RC contributions to the Born level cross section for three energies. We show only the components σ_{-+} and σ_{+-} because even in cases of a partly polarized initial state, the polarized cross sections are mainly determined by these components.

It is seen that for the c.m. energies (5), the weak relative corrections for mostly positive electron polarization are positive and have very low energy dependence. For $(P_{e^+}, P_{e^-}) = (-1, +1)$ they are practically constant.

In the case of mostly negative electron polarization, the weak relative corrections are negative and highly energy dependent.

The QED relative corrections strongly depend on the energy and very weakly on the degree of initial beam polarizations.

To estimate theoretical uncertainty, we carry out calculations in two EW schemes. The integrated cross sections for the weak corrections in the $\alpha(0)$ and G_μ schemes and their relative differences

$$\delta_{G_\mu/\alpha(0)} = \frac{\sigma_{G_\mu}}{\sigma_{\alpha(0)}} - 1, \% \tag{7}$$

are presented in Table III.

As is well known, the difference between two EW schemes in the LO is just the ratio of the EW couplings and gives $\delta^{\rm LO}_{G_\mu/\alpha(0)} = 7.5\%$. As seen in the table, the weak contribution reduces the difference to about 1% at the energy of 250 GeV, 0.7% at 500 GeV, and 0.4% at 1000 GeV. These ratios (7) show stabilization of the results and can be considered as an estimation of the theoretical uncertainty of weak contributions, which is in line with additional corrections of two and more loops.

C. Multiple photon ISR relative corrections

We evaluate ISR corrections to high-energy processes in the channel electron-positron annihilation within the LLA

TABLE III. Integrated Born and weak contributions to the cross section corrections in two EW schemes, $\alpha(0)$ and G_μ, at the c.m. energies (5).

$\sqrt{s}$, GeV	250	500	1000
$\sigma^{\rm Born}_{\alpha(0)}$, pb	1.0198(1)	0.38530(1)	0.14044(1)
$\sigma^{\rm Born}_{G_\mu}$, pb	1.0961(1)	0.41412(1)	0.15095(1)
$\delta^{\rm Born}_{G_\mu/\alpha(0)}$, %	7.48(1)	7.48(1)	7.48(1)
$\sigma^{\rm weak}_{\alpha(0)}$, pb	1.0227(1)	0.37663(1)	0.13381(1)
$\sigma^{\rm weak}_{G_\mu}$, pb	1.0323(1)	0.37914(1)	0.13433(1)
$\delta^{\rm weak}_{G_\mu/\alpha(0)}$, %	0.94(1)	0.66(1)	0.39(1)

TABLE IV. Multiple photon ISR relative corrections δ (%) in the LLA approximation the set c.m. energies (5).

$\sqrt{s}$, GeV	250	500	1000
$\mathcal{O}(\alpha L)$, γ	−2.436(1)	+8.074(1)	+13.938(1)
$\mathcal{O}(\alpha^2 L^2)$, γ	−0.692(1)	−0.268(1)	+0.229(1)
$\mathcal{O}(\alpha^2 L^2)$, e^+e^-	−0.013(1)	+0.324(1)	+1.516(1)
$\mathcal{O}(\alpha^2 L^2)$, $\mu^+\mu^-$	−0.008(1)	+0.199(1)	+0.958(1)
$\mathcal{O}(\alpha^3 L^3)$, γ	+0.034(1)	−0.014(1)	−0.016(1)
$\mathcal{O}(\alpha^3 L^3)$, e^+e^-	−0.017(1)	−0.022(1)	−0.051(1)
$\mathcal{O}(\alpha^3 L^3)$, $\mu^+\mu^-$	−0.010(1)	−0.013(1)	−0.033(1)
$\mathcal{O}(\alpha^4 L^4)$, γ	< 0.001	< 0.001	< 0.001

using the QED structure function formalism [8]. For corrections of this kind the large logarithm corresponds to $L = \ln(s/m_e^2)$, where the total c.m. energy $\sqrt{s}$ is chosen as the factorization scale. In Table IV we show the ISR corrections of different order of $\mathcal{O}(\alpha^n L^n), n = 2-3$ in the leading logarithmic approximation for the c.m. energies (5) in the $\alpha(0)$ EW scheme. To illustrate the trends of the ISR contribution behavior, we present separate distributions for each $\mathcal{O}(\alpha^n L^n)$ term. When considering corrections in LLA, we see that it is certainly sufficient to take into account corrections up to the third order. It is seen that the corrections for the sum of all considered orders of the ISR terms $\sum_{n=2}^{3} \mathcal{O}(\alpha^n L^n)$ are about −0.706% for the c.m. energy $\sqrt{s} = 250$ GeV and about +0.206% (+2.603%) for the c.m. energy $\sqrt{s} = 500(1000)$ GeV. For the c.m. energy $\sqrt{s} = 250$ GeV the most significant contribution in LLA is of course the photonic one of the order $\mathcal{O}(\alpha^2 L^2)$. For the c.m. energy $\sqrt{s} = 500\,(1000)$ GeV the dominant contributions of the second order are about +0.324% (1.516%) for e^+e^- pairs.

D. Differential distributions

1. Angular dependence

Figures 4–6 show the angular dependence of the unpolarized cross sections [Born and one-loop level in the $\alpha(0)$ EW scheme] as well as QED and weak relative corrections. The ϑ_Z is the angle between the initial positron $e^+(p_1)$ and any Z boson.

For all c.m. energies the minimum of the Born and one-loop cross sections is at zero (the dependence is symmetric about zero) while the maximum is in the corners $\cos\vartheta_Z = \pm 1$.

At $\sqrt{s} = 250$ GeV the QED relative corrections dominate and only slightly change by weak corrections. At $\sqrt{s} = 500$ and 1000 GeV both corrections are large and a strong compensation occurs.

2. Energy dependence

The LO and NLO EW corrected unpolarized cross sections and the relative corrections in the parts (QED

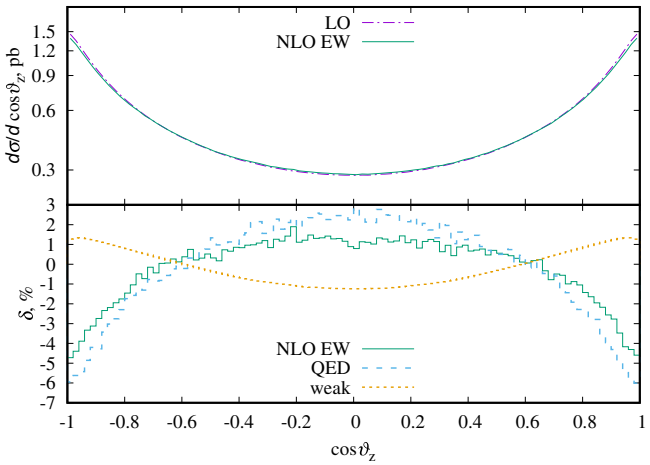

FIG. 4. LO and EW NLO (in parts) cross sections and relative corrections at $\sqrt{s} = 250$ GeV for unpolarized initial beams.

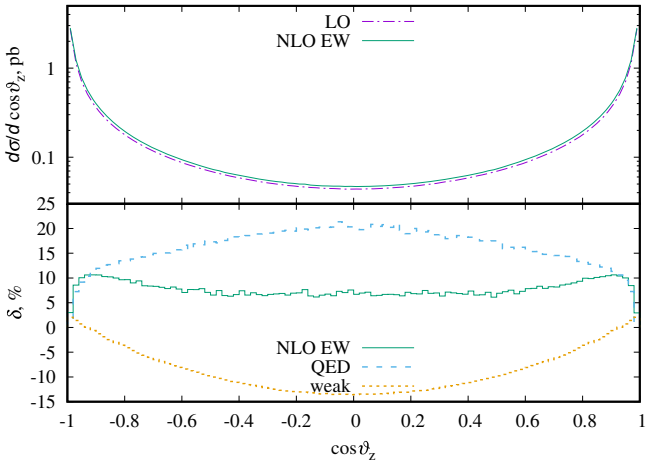

FIG. 5. The same as in Fig. 4 but for $\sqrt{s} = 500$ GeV.

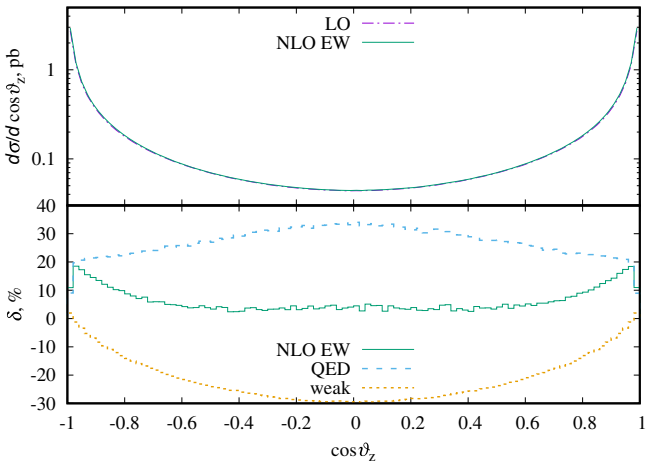

FIG. 6. The same as in Fig. 4 but for $\sqrt{s} = 1000$ GeV.

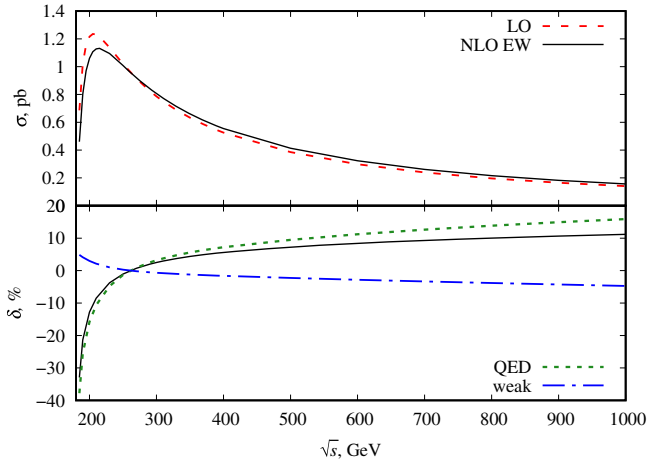

FIG. 7. The LO and NLO EW corrected unpolarized cross sections and the relative corrections in parts as a function of the c.m. energy.

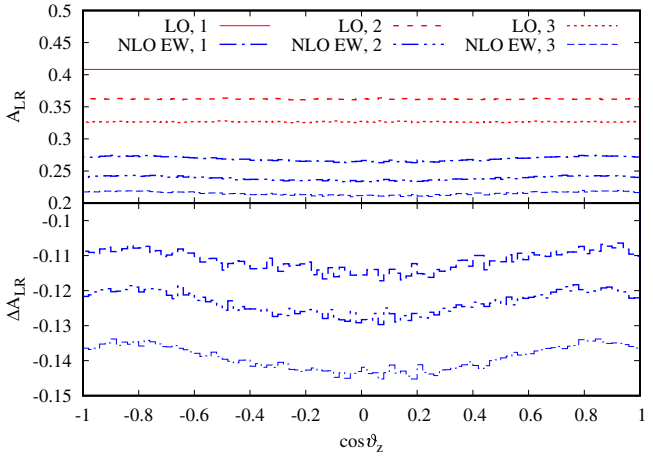

FIG. 8. The asymmetry A_{LR} in the Born and one-loop approximations at c.m. energy $\sqrt{s} = 250$ GeV for fully polarized and partially polarized initial beams vs the cosine of the scattering angle.

and weak) as a function of the c.m. energy are shown in Fig. 7.

In the c.m. energy range from the threshold to 1000 GeV, the QED corrections dominate except for the point near $\sqrt{s} = 260$–270 GeV, where the QED and weak corrections are equal to each other. Below this point, the total relative corrections are negative, then become positive and reach about 10% at $\sqrt{s} = 1000$ GeV.

E. Asymmetries

All one-loop corrections for this process are symmetric in the $u \leftrightarrow t$ exchange, so that there is no forward-backward asymmetry which could be more easily observed without polarization.

The left-right asymmetry A_{LR} for the fully polarized case is defined as follows:

$$A_{\mathrm{LR}} = \frac{\sigma_{\mathrm{LR}} - \sigma_{\mathrm{RL}}}{\sigma_{\mathrm{LR}} + \sigma_{\mathrm{LL}} + \sigma_{\mathrm{RL}} + \sigma_{\mathrm{RR}}}, \tag{8}$$

since to cross section $\sigma_{\mathrm{LL,RR}}$ only hard real photons account, and σ_{LR} and σ_{RL} are the cross sections for the fully polarized electron-positron $e^-_{\mathrm{L}}e^+_{\mathrm{R}}$ and $e^-_{\mathrm{R}}e^+_{\mathrm{L}}$ initial states, respectively.

In the case of partially polarized initial beams, the asymmetry can be written as

$$A_{\mathrm{LR}} = \frac{\sigma(P_{e^+}, P_{e^-}) - \sigma(-P_{e^+}, -P_{e^-})}{\sigma(P_{e^+}, P_{e^-}) + \sigma(-P_{e^+}, -P_{e^-})}. \tag{9}$$

At the Born level A_{LR} is constant [4].

In Figs. 8–10 the left-right asymmetry distributions for Born and one-loop contributions are shown as a function of the cosine scattering angle for the c.m. energies (5) in the $\alpha(0)$ EW scheme. The (1) stands for the fully polarized case, while (2) stands for the partially polarized case with

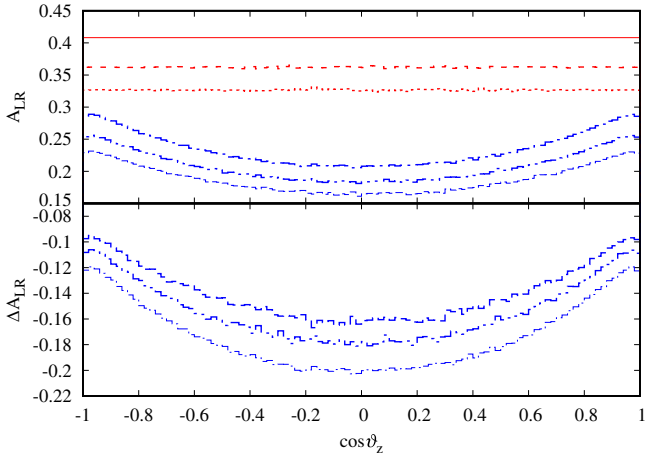

FIG. 9. The same as in Fig. 8 but for c.m. energy $\sqrt{s} = 500$ GeV.

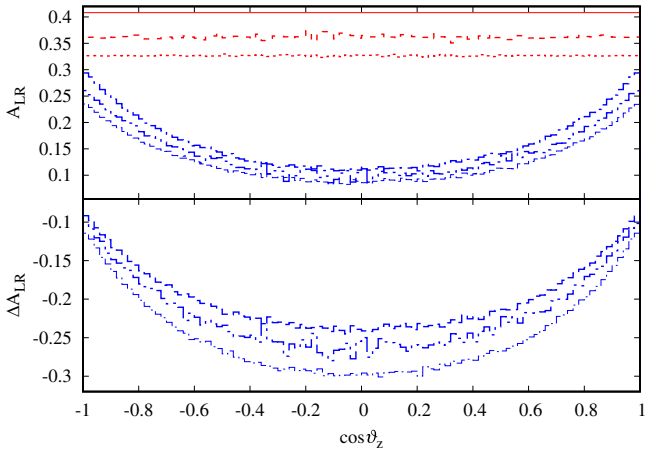

FIG. 10. The same as in Fig. 8 but for c.m. energy $\sqrt{s} = 1000$ GeV.

TABLE V. Integrated Born and one-loop cross sections for unpolarized initial beams at the c.m. energy $\sqrt{s} = 250$ GeV for $e^+e^- \to ZZ \overset{\text{n.w.}}{\to} 2\mu^+2\mu^-$ channel.

P_{e^+}, P_{e^-}	0, 0	−1, +1	+1, −1	+0.3, −0.8	−0.3, +0.8	0, −0.8	0, +0.8
σ^{Born}, fb	1.0730(1)	1.2700(1)	3.0220(1)	1.8123(1)	0.8487(1)	1.4235(1)	0.7226(1)
σ^{NLO}, fb	1.1250(1)	1.6414(1)	2.8579(1)	1.7296(1)	1.060(1)	1.3685(1)	0.8818(1)
δ^{NLO}, %	4.85(1)	29.25(1)	−5.43(1)	−4.57(1)	24.95(1)	−3.86(1)	22.04(1)
$\delta^{\text{NLO}}_{\text{lin}}$, %	4.83(1)	27.84(1)	−4.87(1)	−4.06(1)	23.79(1)	−3.39(1)	21.05(1)

$(P_{e^+}, P_{e^-}) = (+0.3, -0.8)$, and (3) stands for $(P_{e^+}, P_{e^-}) = (0, -0.8)$. The corresponding shift of the asymmetry,

$$\Delta A_{\text{LR}} = A_{\text{LR}}(\text{NLO EW}) - A_{\text{LR}}(\text{LO}),$$

is shown in the lower panel.

We observe a symmetric behavior of A_{LR} with respect to $\cos\vartheta_Z = 0$, the significant dependence on energy, the flatter behavior with decreasing energy, and the large sensitivity to electroweak interaction effects the degree of the initial beam polarization.

F. Narrow-width approximation for the decay channel

In this approach we create a narrow-width cascade using Born and one-loop $e^+e^- \to ZZ$ and $Z \to \mu^+\mu^-$ formulas, i.e.,

$$\sigma^{\text{LO,NLO}}_{e^+e^-\to 2\mu^+2\mu^-} = \sigma^{\text{LO,NLO}}_{e^+e^-\to ZZ}\,\text{Br}^{\text{LO,NLO}}_{Z\to\mu^+\mu^-}\,\text{Br}^{\text{LO,NLO}}_{Z\to\mu^+\mu^-}, \tag{10}$$

where Br is a partial branching factor

$$\text{Br}^{\text{LO,NLO}}_{Z\to\mu^+\mu^-} = \frac{\Gamma^{\text{LO,NLO}}_{Z\to\mu^+\mu^-}}{\Gamma_Z}. \tag{11}$$

At one-loop, it is more consistent to use instead its "linearized" version

$$\sigma^{\text{NLO}}_{e^+e^-\to 2\mu^+2\mu^-} = \sigma^{\text{LO}}_{e^+e^-\to ZZ}\text{Br}^{\text{LO}}_{Z\to\mu^+\mu^-}(1 + \delta_{e^+e^-\to ZZ} + 2\delta_{Z\to\mu^+\mu^-}). \tag{12}$$

The partial width for $Z \to \mu^+\mu^-$ decay at the LO and NLO levels are $\Gamma^{\text{Born}} = 80.9363$ MeV, $\Gamma^{\text{NLO}} = 83.3286$ MeV, ($\delta_{Z\to\mu^+\mu^-} = 2.956\%$) and the corresponding branching factors are: $\text{Br}^{\text{LO}}_{Z\to\mu^+\mu^-} = 0.032437$, $\text{Br}^{\text{NLO}}_{Z\to\mu^+\mu^-} = 0.033396$.

Since the narrow-width approximation is valid at the c.m. energy of the reaction threshold $\sqrt{s} = 2M_Z \approx 182$ GeV, the only lowest energy $\sqrt{s} = 250$ GeV of the accelerators is given in Table V.

To obtain the differential distributions as well as final lepton polarization, full off-shell/double-pole approximation calculations should be carried out.

IV. CONCLUSION

In this paper we have described the evaluation of polarization effects for the cross sections of the Z pair productions at the one-loop level at high energies.

Comparisons of the results at the tree level for the Born and hard photon bremsstrahlung with CalcHEP [16] and WHIZARD [17,18] are given, and a very good agreement is found. Our numerical results for one-loop contributions fully confirm the results in [4] and do not confirm the results of [6].

The angular and energy dependence with the effect of polarization of the initial states was carefully analyzed for certain helicity states. The polarization effects were found to be significant. The increase of the cross section for mostly negative electron polarization compared to the unpolarized one was found. The radiative corrections themselves were rather sensitive to degrees of polarization of the initial beams and depended quite strongly on energy.

In addition, calculations in the $\alpha(0)$ and G_μ EW schemes were considered. The results for relative corrections in the G_μ EW scheme are approximately 5%–6% less than in the $\alpha(0)$ one. The difference between complete one-loop cross sections in the considered EW schemes is about 1% or less. This could be regarded as a theoretical uncertainty.

ACKNOWLEDGMENTS

The research was supported by the Russian Science Foundation, Project No. 22-12-00021.

[1] S. Bondarenko, Y. Dydyshka, L. Kalinovskaya, L. Rumyantsev, R. Sadykov, and V. Yermolchyk, Phys. Rev. D **100**, 073002 (2019).
[2] A. Arbuzov, S. Bondarenko, L. Kalinovskaya, R. Sadykov, and V. Yermolchyk, Symmetry **13**, 1256 (2021).
[3] S. Bondarenko, Ya. Dydyshka, L. Kalinovskaya, L. Rumyantsev, R. Sadykov, and V. Yermolchyk, JETP Lett. **115**, 495 (2022).
[4] A. Denner and T. Sack, Nucl. Phys. **B306**, 221 (1988).
[5] G. J. Gounaris, J. Layssac, and F. M. Renard, Phys. Rev. D **67**, 013012 (2003).
[6] M. Demirci and A. B. Balantekin, Phys. Rev. D **106**, 073003 (2022),
[7] D. Bardin, S. Bondarenko, L. Kalinovskaya, G. Nanava, L. Rumyantsev, and W. von Schlippe, Comput. Phys. Commun. **177**, 738 (2007).
[8] E. A. Kuraev and V. S. Fadin, Sov. J. Nucl. Phys. **41**, 466 (1985).
[9] Z. Nagy and D. E. Soper, J. High Energy Phys. 07 (2008) 025.
[10] Z. Nagy and D. E. Soper, J. High Energy Phys. 06 (2014) 097.
[11] D. R. Yennie, S. C. Frautschi, and H. Suura, Ann. Phys. (N.Y.) **13**, 379 (1961).
[12] S. Jadach, B. F. L. Ward, and Z. Was, Phys. Lett. B **449**, 97 (1999),
[13] D. Y. Bardin, D. Lehner, and T. Riemann, Nucl. Phys. **B477**, 27 (1996),
[14] S. Jadach, W. Placzek, and B. F. L. Ward, Phys. Rev. D **56**, 6939 (1997),
[15] A. Denner, S. Dittmaier, and M. Roth, Phys. Lett. B **429**, 145 (1998),
[16] A. Belyaev, N. D. Christensen, and A. Pukhov, Comput. Phys. Commun. **184**, 1729 (2013).
[17] W. Kilian, T. Ohl, and J. Reuter, Eur. Phys. J. C **71**, 1742 (2011).
[18] W. Kilian, S. Brass, T. Ohl, J. Reuter, V. Rothe, P. Stienemeier, and M. Utsch, arXiv:1801.08034.
[19] R. Sadykov and V. Yermolchyk, Comput. Phys. Commun. **256**, 107445 (2020).
[20] G. Moortgat-Pick *et al.*, Phys. Rep. **460**, 131 (2008).
[21] D. Bardin, L. Kalinovskaya, A. Arbuzov, S. Bondarenko, P. Christova *et al.*, Proc. Sci. ACAT (**2007**) 077.
[22] D. Y. Bardin and G. Passarino, arXiv:hep-ph/9803425.
[23] A. Denner and S. Dittmaier, Phys. Rep. **864**, 1 (2020).
[24] A. Bredenstein, A. Denner, S. Dittmaier, and M. M. Weber, Phys. Rev. D **74**, 013004 (2006),